JOURNAL OF GUIDANCE, CONTROL, AND DYNAMICS
Vol. 20, No. 5, September–October 1997

More on Gain Adaptive Tracking

D. D. Sworder* and J. E. Boyd†
University of California, San Diego, La Jolla, California 92093-0407

Tracking an agile target is made difficult by a multiplicity of possible motion modes. An earlier paper (Sworder, D. D., Vojak, R., and Hutchins, R. G., "Gain Adaptive Tracking," *Journal of Guidance, Control, and Dynamics*, Vol. 16, No. 5, 1993, pp. 865–873) described how measurements of the spatially extended features of the target can be used to create a tracker that can follow a jinking motion. The earlier algorithm is extended to include discontinuities in the target path. The tracker is only slightly more complex than that for continuous paths. The response of the proposed tracker is shown by example to be superior to both an extended Kalman filter and the earlier gain adaptive tracker.

I. Introduction

THE requirement that a maneuvering target be tracked with good accuracy is a part of many system applications. This can be a particularly formidable problem because the model dynamics may be nonlinear and have a peculiar geometric structure. Consider an agile target moving at nearly constant speed and maneuvering by jinking. If the accelerations of the target are represented by continuous processes, considerable effort has been expended utilizing the extended Kalman filter (EKF) framework including representing the maneuver acceleration by increasing the variance of the Brownian excitation of the target (pseudonoise)[1] and representing the maneuver acceleration with a linear Gauss–Markov (LGM) surrogate (colored noise).[2] But studies have shown maneuvers to be more closely modeled by a piecewise constant random process, and it is very difficult to represent the effect of abrupt changes in the motion mode with a diffusion. Other authors have employed a set of parallel linear models (the multiple model approach) to delineate the various maneuver modes, one for each mode [for noncommunicating models see Ref. 3, and for communicating models see the interacting multiple model (IMM) of Blom and Bar-Shalom[4]]. Particularly, the IMM has shown a good ability to improve performance with restricted computational complexity. In benchmark tests, the IMM proved superior to several other multimodal approaches.[5]

Several authors have examined alternative approaches to the agile target tracking problem using novel sensor architectures. For example, a range-bearing measurements (a radar) can be augmented with an image measurement processed to yield target orientation and/or target type. From changes in orientation, a turn can be detected, and from type information, the proper dynamics of target evolution can be determined.[6] Maneuver status and target type are modal variables and, in combination with the conventional target states, give the comprehensive state description of the target. An algorithm that integrates the outputs of disparate sensors into an effective estimate of the current (mode × location) state of the target is difficult to produce; the output of a modal sensor/processor is a classification and the radar output is a point. It is hard to meld measurements with such different formats. Of course, a separation can be imposed in which the modal measurements are used for classification and the point measurements are interpreted within the context provided by the ostensible classification.

Better performance results when the diverse sensors are integrated in an eclectic manner.[7] The basic problem can be described as follows. For notational convenience, in what follows $\boldsymbol{S}$ will designate an integer index set $\{1, \ldots, S\}$; $\boldsymbol{e}_i$ is the ith canonical unit vector in a space whose dimension is obvious from the context with $\boldsymbol{E}_i = \boldsymbol{e}_i \boldsymbol{e}_i'$, $\mathbf{1}$ is a vector of ones, and $\mathbf{N}(x, P)$ is a Gaussian density with (mean, covariance) equal to (x, P). Where no confusion will arise, a subscript may identify time, the component of a vector, a particular set of components of a vector, e.g., $\{\nu_1\}$ is a scalar process that is the first component of the vector process $\{\nu_t\}$, whereas $\{\nu_x\}$ is a set of processes in $\{\nu_t\}$ associated with $\{x_t\}$; the integrands in stochastic differential equations will be understood to be predictable versions of the associated right continuous, random processes, e.g., ϕ_i is actually the inner product $\langle \boldsymbol{e}_i, \phi_{t-} \rangle$ in Eq. (1′); an asterisk is the Hadamard product $[(x * y)_i = x_i y_i]$; and $A \otimes B$ is the Kronecker product of a matrix A and a matrix B. Suppose the modal state is an indicator process $\{\phi_t\}$ with state space the s canonical unit vectors in $\Re^s$; i.e., $\phi_t = \boldsymbol{e}_i$; $i \in \boldsymbol{S}$ indicates that the ith modal condition is true at time t. The base states of the target, e.g., position and velocity of a point-equivalent target, satisfy the differential equation

$$\mathrm{d}x_t = \sum_{i \in \boldsymbol{S}} A_i x_t \phi_i \, \mathrm{d}t + \mathrm{d}w_t \tag{1′}$$

where $\{w_t\}$ is a Brownian motion, $E\{w_t w_t'\} = Wt$. For fixed ϕ_t, Eq. (1′) is the conventional motion model used in tracking [see, for example, Eq. (1) of Ref. 8 for the analog of Eq. (1′) in discrete time]. The base-state dynamics of the target change in concert with the modal state. The modal process is an index process and is most commonly depicted as a Markov process,

$$\mathrm{d}\phi_t = Q' \phi_t \, \mathrm{d}t + \mathrm{d}m_t \tag{2}$$

where $\{m_t\}$ is a discontinuous martingale.

The base state is usually identified with the orthodox state vector, whereas the modal state is a regime indicator and designates the appropriate parameterization of the equation of base-state evolution. Were it not for the dependence on $\{\phi_t\}$, Eq. (1′) would generate Gaussian sample paths. The primary effect of the modal state is to modulate the base-state dynamics by changing the form of the $\{A_t\}$ process

$$A_t = \sum_i A_i \phi_i$$

so as to cause it to correspond to changing exogenous conditions. The comprehensive state of the target includes both elements, $\{x_t, \phi_t\}$. (The modal state is also called the metastate by Friedland[9] when used in the context of adaptive control.)

The form of the state estimator is dependent on the quality and type of the measurements. These measurements in turn depend on the configuration of sensors in the application. In the classical situation, there is a base-state observation given by

$$\mathrm{d}y_t = Dx_t \, \mathrm{d}t + \mathrm{d}n_x \tag{3}$$

with $y_0 = 0$; $\{n_x\}$ is a Brownian motion with quadratic variation $R_x t$ ($R_x > 0$), independent of the exogenous processes in Eqs. (1′) and (2). If the measurement occurs at a discrete set of times, the

Received June 10, 1996; revision received April 2, 1997; accepted for publication May 16, 1997. Copyright © 1997 by the American Institute of Aeronautics and Astronautics, Inc. All rights reserved.

*Professor, Department of Electrical and Computer Engineering, and Acting Vice Chancellor for Research. E-mail: dsworder@ucsd.edu.

†Research Assistant, Department of Electrical and Computer Engineering; currently Senior Systems Scientist, Cubic Defense Systems, 9233 Balboa, San Diego, CA 92123. E-mail: john.boyd@cubic.com.

analogous base-state observation is $y_k = Dx_k + n_k$. Denote the filtration generated by $\{y_t, \phi_t\}$ by $\{\hat{\boldsymbol{G}}_t\}$. The Kalman filter (KF) (or EKF in certain nonlinear problems) generates the $\hat{\boldsymbol{G}}_t$ conditional mean of $\{x_t\}$. The KF is phrased in terms of an equation for $\{\hat{x}_t\}$ and an equation for a single canonical higher moment P_{xx}, the error covariance. For discrete observations, the KF is given as follows.

Between measurements,

$$\frac{\mathrm{d}}{\mathrm{d}t}\hat{x}_t = \sum_i A_i \hat{x}_t \phi_i$$
$$\frac{\mathrm{d}}{\mathrm{d}t}P_{xx} = \sum_i A_i P_{xx}\phi_i \sum_i P_{xx}A_i'\phi_i + W \tag{4}$$

At a measurement,

$$\Delta\hat{x}_t = \gamma_x \Delta\nu_x \qquad \Delta P_{xx} = -\gamma_x(DP_{xx}D' + R_x)\gamma_x' \tag{5}$$

subject to appropriate initial conditions, where $\gamma_x = P_{xx}D'(DP_{xx}D' + R_x)^{-1}$ (the orthodox Kalman gain) and $\Delta\nu_x = y_t - D\hat{x}_t$ (the innovations process). The modal process must be known (or measured) to implement this algorithm. Indeed, $\{P_{xx}\}$ is random only because it is contingent on the path of $\{\phi_t\}$.

The issues that arise in tracking are clearer when phrased in the context of a specific model. Consider the problem of tracking the motion of an agile object in the X–Y plane. A simple model for an evasive target moving at essentially constant speed is given by the following fourth-order equation:

$$\mathrm{d}\begin{pmatrix} X \\ Y \\ V_x \\ V_y \end{pmatrix} = \begin{bmatrix} 0 & 0 & 1 & 0 \\ 0 & 0 & 0 & 1 \\ 0 & 0 & 0 & -\omega \\ 0 & 0 & \omega & 0 \end{bmatrix}\begin{bmatrix} X \\ Y \\ V_x \\ V_y \end{bmatrix}\mathrm{d}t + \begin{bmatrix} 0 & 0 \\ 0 & 0 \\ 1 & 0 \\ 0 & 1 \end{bmatrix}\mathrm{d}\begin{pmatrix} w_x \\ w_y \end{pmatrix} \tag{6}$$

where $\{X, Y\}$ are position coordinates and $\{V_x, V_y\}$ are associated velocities. The target is subject to two types of acceleration: a wideband omnidirectional acceleration described by the Brownian motion $\{w_x, w_y\}$ and a maneuver acceleration represented by the turn rate process $\{\omega\}$. The latter is troublesome in two respects. First, because of its temporal structure, the sample paths of the maneuver accelerations are better described by a discontinuous rather than a continuous process and are clearly non-Gaussian.[10] Second, the target dynamics are indexed by the turn rate and, consequently, are polymorphic. A useful maneuver model is created by partitioning the range of turn rates into K levels: $\omega \in \{a_1, \ldots, a_K\}$ (Refs. 11 and 12). Let $\{\alpha_t\}$ be the maneuver indicator process, $\alpha_t = \boldsymbol{e}_i$ if $\omega = a_i$ at time t, and suppose $\{\alpha_t\}$ is well represented as a Markov process.

Altered measurement architectures have been proposed.[13] An image-based measurement of spatially extended features of the target was provided to the estimator as a complement to the base-state measurement. For example, an image processor might give an indication of both the current orientation of the target from an analysis of the silhouette and a direct classification of the maneuver mode from a peculiarity of the radiation pattern within the image. The modal sensor is typically a feature matching block, and its errors are not well described by additive Gaussian noise. Specifically, partition the orientation field into L angular bins of width $2\pi/L$, and let the orientation indicator process be given by $\{\rho_t\}$: $\rho_t = \boldsymbol{e}_i$ if the current target orientation is in the ith bin. The maneuver state of the target is given by $\{\phi_t\} = \{\alpha_t \otimes \rho_t\}$, the Kronecker product of maneuver and orientation. Under such conditions, $\{\phi_t\}$ can be represented by Markov process, the method of construction of which is given in detail in Ref. 13.

To create realistic model of the modal classifier, suppose that the sensor collects and classifies data at a rate of λ frames/s. Each measurement is placed into one of the KL modal bins. The quality of the modal sensor/processor is determined by the $KL \times KL$ discernibility matrix $\mathbf{P} = [\mathbf{P}_{ij}]$, where $\mathbf{P}_{ij}$ is the probability that modal bin i will be selected by the processor if modal bin j contains the true maneuver mode at the time of measurement, i.e., $\mathbf{P}_{ij} = \mathcal{P}(\Delta\sigma_i = 1 \mid \phi = e_j)$ (Ref. 14). The output of the processor can be written as a KL-dimensional counting process $\{\sigma_t\}$, the ith component of which is the number of times the target has been placed in bin i on the interval $[0, t]$. This sequence of counts (or symbols) can be interpreted by a temporal processor to give the relative likelihoods of the various maneuver hypotheses. This development was carried out in Ref. 13 under the assumption that only angular orientation was measured.

The capacity for modal inference is a function of three things: the sample rate λ, the ability of the modal sensor to classify correctly a single measurement $\mathbf{P}$, and the tempo of modal variation Q. Denote the filtration generated by the modal sensor by $\{\boldsymbol{Z}_t\}$, and denote the filtration generated by both sensors by $\{\boldsymbol{G}_t\}$ (in contrast to $\{\hat{\boldsymbol{G}}_t\}$, which contains perfect modal observations). Clearly, if the fidelity of the modal sensor is such that $\{\phi_t\}$ can be determined with good accuracy, estimation of $\{x_t\}$ reduces to the KF with $\{\phi_t\}$ replaced by its σ_t-based estimate. The solution to the more general tracking problem involves finding the $\boldsymbol{G}_t$ expectation of $\{x_t, \phi_t\}$.

The advantages of modal measurement were noted early on in various contexts, although the problem was typically studied within an EKF framework.[15] In Ref. 13 a nonlinear processing algorithm, the polymorphic estimator (PME), was proposed. [This was labeled EKF_A in Ref. 13, Eqs. (9–14).] Because of the nonlinear, non-Gaussian nature of Eqs. (1′) and (2), the development of an exact, finite dimensional, recursive algorithm for generating the $\boldsymbol{G}_t$ conditional mean of the comprehensive state seems not to be possible. In Ref. 13, an approximation to $\{\hat{x}_t, \hat{\phi}_t\}$ was developed under the assumption that most of the information about ϕ_t is conveyed by the modal observations; specifically, when a $\hat{\boldsymbol{G}}_t$ predictable process is independent of $\{y_t\}$, it is assumed that the direct contribution of the $\boldsymbol{G}_t$ innovations due to $\{y_t\}$ is small as compared to that due to $\{\sigma_t\}$. The PME has a form similar to the KF but requires the computation of three canonical higher moments instead of the single moment required in the KF, and these canonical moments depend on the modal measurements.

The jinking path presented in Eq. (1′) is one example of an evasive motion: the target turns so as to make its path difficult to predict. If $\{y_t\}$ is generated by a radar, an agile target will maneuver so as to get outside the radar window, i.e., cause loss of lock (LOL). To avoid LOL, the sample rate or the signal-to-noise ratio (SNR) of the radar must be increased. To increase the likelihood of LOL, the target may execute more complex motions than those provided for in Eq. (1′). Of particular interest are motions that combine turns with abrupt state changes; suppose the motion dynamics are given by

$$\mathrm{d}x_t = \sum_i A_i\phi_i x_t\,\mathrm{d}t + \rho'\,\mathrm{d}\phi + \sum_i B_i\phi_i\,\mathrm{d}w_t \tag{1}$$

with initial condition x_0, $\{x_0$ is $\mathbf{N}[0, P_{xx}(0)]\}$. Equation (1) generalizes (1′) in two ways: 1) the process noise is subject to a mode dependent amplification, and 2) there is a base-state discontinuity when $\{\phi_t\}$ changes; if ϕ_t goes $i \to \ell$, $\Delta x_t = \rho_{\ell\cdot} - \rho_{i\cdot}$.

In this paper, the PME is revisited. It is shown that a modification of the algorithm, polymorphic estimator modification (PMEM), provides improved performance in the presence of discontinuities using the earlier estimation structure. The moments that need be calculated are the same as those in the PME, but the changes in Eq. (1) give rise to slightly different extrapolation equations. The paper concludes with an example of a sample path of an evasive target. The performance of the PMEM is contrasted with the PME and a conventional EKF. It is shown that PMEM has generally better tracking performance and a more accurate view of its performance.

II. PMEM

The Appendix gives a succinct development of the PMEM algorithm. Define the vector mean observation rate $\boldsymbol{\lambda}_t = \lambda\mathbf{P}\phi_t$: the ith component of $\boldsymbol{\lambda}_t$ is the expected rate of receiving the ith observation for a given maneuver state. The PMEM update at a modal measurement is most concisely written in terms of $\{\vartheta_t\}$, a piecewise constant process with increments $\Delta\vartheta_t = \lambda\mathbf{P}'(\hat{\boldsymbol{\lambda}}_t^{-1} * \Delta\sigma_t)$, where $\hat{\boldsymbol{\lambda}}_t^{-1}$ is to be interpreted componentwise. The PMEM is given by the composition of the PMEM-maneuver filter and the PMEM-translation filter.

PMEM-Maneuver Filter

Between observations,

$$\frac{\mathrm{d}}{\mathrm{d}t}\hat{\phi}_t = Q'\hat{\phi}_t \tag{7a}$$

At a modal measurement,

$$\hat{\phi}^+ = \hat{\phi}^- * \Delta\vartheta \tag{7b}$$

subject to an appropriate initial condition. This equation is identical to Eq. (9) of Ref. 13, with a change in notation.

The estimates of position and velocity are given by the PMEM-translation filter. This algorithm has a conventional form, mapping the point measurements into an estimate of the base state, with gains that are functions of both the modal and the point measurements.

PMEM-Translation Filter

Between observations,

$$\frac{\mathrm{d}}{\mathrm{d}t}\hat{x}_t = \sum_i A_i (R_{x\phi})_{\cdot i} + \rho' Q' \hat{\phi}_t \tag{8a}$$

At a motion measurement,

$$\Delta\hat{x}_t = \gamma_x \Delta\nu_x \tag{8b}$$

At a modal measurement,

$$\Delta\hat{x}_t = P_{x\phi}\Delta\vartheta \tag{8c}$$

where γ_x and ν_x are given in the KF and $R_{x\phi} = P_{x\phi} + \hat{x}\hat{\phi}'$. P_{xx} and $P_{x\phi}$ are the (random) second central moments of the estimation error. Equation (8) is similar to Eq. (10) of Ref. 13, with differences to be noted in what follows.

The calculation of $\{\hat{x}_t\}$ requires the same three canonical moments found in Ref. 13: the aforementioned P_{xx} and $P_{x\phi}$ along with a third central mixed moment associated with $xx'\phi$ labeled $\{\pi_{xx}(m); m \in \boldsymbol{KL}\}$. The equation of evolution for the canonical moments (to follow) is given in Eq. (9). The Ξ_i factors are algebraic functions of the canonical moments. They appear in expanded from in Eqs. (11–14) in Ref. 13 and are also given in the Appendix. Denote $B_i B_i' = W_i$. Equation (9) contains moments of the $\{m_t\}$ process not appearing in the PME: $\boldsymbol{V}$ is the predictable quadratic variation of $\{m_t\}$ and $\boldsymbol{U}$ is a predictable cubic variation. The equations for both are given in the Appendix.

PMEM-Translation Moments

Between observations,

$$\begin{aligned}
\frac{\mathrm{d}}{\mathrm{d}t}P_{xx} &= \left[\sum_i A_i \Xi_2(i) + \rho' Q' P_{\phi x}\right] + [\cdots]' \\
&\quad + \sum_i W_i \hat{\phi}_i + \sum_r \rho' \boldsymbol{V}(\boldsymbol{e}_r)\hat{\phi}_r \rho \\
\frac{\mathrm{d}}{\mathrm{d}t}P_{x\phi} &= \sum_i A_i \Xi_4(i) + \rho'\left[Q' P_{\phi\phi} + \sum_i \boldsymbol{V}(\boldsymbol{e}_i)\hat{\phi}_i\right] + P_{x\phi} Q \\
\frac{\mathrm{d}}{\mathrm{d}t}\pi_{xx}(m) &= \left\{\sum_i A_i \Xi_5(i,m) + \rho'\left[\sum_i \boldsymbol{V}(\boldsymbol{e}_i)_{\cdot m}(P_{\phi x})_{i\cdot}\right.\right. \\
&\quad \left.\left. + Q'\pi_{\phi x}(m)\right]\right\} + [\cdots]' + \sum_i [\pi_{xx}(i) Q_{im} + (P_{\phi\phi})_{im} W_i] \\
&\quad + \sum_i \rho'[\boldsymbol{V}(\boldsymbol{e}_i)(P_{\phi\phi})_{im} + \boldsymbol{U}_m(\boldsymbol{e}_i)\hat{\phi}_i]\rho
\end{aligned} \tag{9a}$$

At a motion measurement,

$$\begin{aligned}
\Delta P_{xx} &= -\gamma_x (D P_{xx} D' + R_x)\gamma_x' \\
\Delta P_{x\phi} &= -\gamma_x (D P_{xx} D' + R_x)\gamma_\phi' \\
\Delta\pi_{xx}(m) &= -\{\gamma_x D\pi_{xx}(m) + [\gamma_x D\pi_{xx}(m)]'\}
\end{aligned} \tag{9b}$$

At a modal measurement,

$$\begin{aligned}
\Delta P_{xx} &= -\Delta\hat{x}\Delta\hat{x}' + \sum_k \pi_{xx}(k)\Delta\vartheta_k \\
\Delta P_{x\phi} &= -\Delta\hat{x}\Delta\hat{\phi}' + \sum_{k\in S} \pi_{x\phi}(k)\Delta\vartheta_k \\
\Delta\pi_{xx}(m) &= -\Delta\hat{\phi}_m \Delta\hat{x}\Delta\hat{x}' - \Delta\hat{\phi}_m P_{xx}^+ - \Delta\hat{x}\left(P_{\phi x}^+\right)_{m\cdot} \\
&\quad - \left[\Delta\hat{x}\left(P_{\phi x}^+\right)_{m\cdot}\right]' + \sum_j \Phi_m(j)\Delta\vartheta(j)
\end{aligned} \tag{9c}$$

Equation (8) gives the state estimator for a tracker with base-state discontinuities. It is interesting to compare Eq. (8) with the KF and also with the PME. The base-state estimator differs from the KF in obvious ways and in one way that is rather subtle. The term

$$\sum_i A_i \hat{x}_t \phi_i$$

in Eq. (4) is replaced by

$$\sum_i A_i (R_{x\phi})_{\cdot i}$$

in Eq. (8), and the term W in Eq. (5) is replaced with

$$\sum_i W_i \hat{\phi}_i$$

in Eq. (9a), a not surprising change given that ϕ_i is not known now. Additionally, the drift in $\hat{x}_t$ contains a term $\rho' Q' \hat{\phi}_t$ to reflect the expected discontinuity. These changes are easily intuited from the form of Eq. (1). A less obvious change from the KF is hidden in γ_x. The factor P_{xx} is not that given in Eq. (5) but is instead that given in Eq. (9); the gain is a function of the modal measurement sequence.

The dynamics of $\{P_{xx}\}$ in the PMEM are again similar to the error covariance of the KF with differences both overt and covert. The replacement of

$$\sum_i A_i P_{xx} \phi_i$$

in Eq. (5) with

$$\sum_i A_i [\pi_{xx}(i) + P_{xx}\hat{\phi}_i + \hat{x}_t (P_{x\phi})'_{\cdot i}]$$

written as

$$\sum_i A_i \Xi_2(i)$$

in Eq. (9a), is not surprising, nor is the addition of the term

$$\sum_r \rho' \boldsymbol{V}(\boldsymbol{e}_r)\hat{\phi}_r \rho$$

The former accounts for the correlation of the modal- and base-state error. The latter has a long history, sometimes being referred to at the white noise equivalent of the jump discontinuity. It reflects the obvious need to account for the sudden change in the base state, and in an LGM framework, the exogenous disturbances are represented as additional white noise. Of course, the terms and updates involving the modal measurement never appear in the KF because the modal state is neglected in the LGM model.

Comparing Eqs. (7–9) with the PME, the influence of the base-state discontinuity can be isolated. First, the update Eqs. (8b), (8c), (9b), and (9c) in the PMEM are identical to those in the PME. The discontinuity enters into the PMEM only in the equations that propagate the moments between measurements.

For P_{xx}, the inclusion of a discontinuity introduces the following terms into the equation for the base-state error covariance:

$$\frac{\mathrm{d}}{\mathrm{d}t}P_{xx} = \cdots + \rho' Q' P_{\phi x} + P_{x\phi} Q\rho + \sum_r \rho' \boldsymbol{V}(\boldsymbol{e}_r)\hat{\phi}_r \rho \tag{10}$$

As mentioned before, one effect of the discontinuity is to increase the intensity of the exogenous state disturbance. The third term

in Eq. (10) reflects this though it is not truly additive because it depends on $\hat{\phi}_t$. The paired terms $\rho' Q' P_{\phi x} + P_{x\phi} Q \rho$ relate the base-state covariance to the modal-state error. Note that, if the modal estimator has a high quality ($\phi_t = \boldsymbol{e}_k \cong \hat{\phi}_t$), Eq. (10) reduces to $(\mathrm{d}/\mathrm{d}t) P_{xx} = \cdots + \rho' \boldsymbol{V}(\boldsymbol{e}_k) \rho$, a near analog to conventional practice.

For $P_{x\phi}$, the mixed moments do not appear in the KF. Comparing the PMEM with the PME, it appears that

$$\frac{\mathrm{d}}{\mathrm{d}t} P_{x\phi} = \cdots + \rho' \left[Q' P_{\phi\phi} + \sum_i \boldsymbol{V}(\boldsymbol{e}_i) \hat{\phi}_i \right] \tag{11}$$

[see Eq. (24a) in Ref. 13]. The change is related to both the frequency of jumps $[Q, \boldsymbol{V}(\boldsymbol{e}_i)]$ and their size ρ. Again suppose that there is a good estimate of the modal state: $\phi_t = \boldsymbol{e}_k \cong \hat{\phi}_t$. In this event, the contribution due to the discontinuity reduces to $(\mathrm{d}/\mathrm{d}t) P_{x\phi} = \cdots + \rho' \boldsymbol{V}(\boldsymbol{e}_k)$.

For $\pi_{xx}(m)$, this third mixed central moment appears in several places in both the PMEM and the PME. It quantifies the relation between modal errors and the base-state covariance; e.g., it appears as the modal-measurement gain in P_{xx} [see Eq. (9)]. Again looking at the terms that depend on the state discontinuity [compare Ref. 13, Eq. (33a)]:

$$\frac{\mathrm{d}}{\mathrm{d}t} \pi_{xx}(m) = \cdots + \rho' \left[\sum_i \boldsymbol{V}(\boldsymbol{e}_i)_{.m} (P_{\phi x})_{i.} + Q' \pi_{\phi x}(m) \right]$$

$$+ [\cdots]' + \sum_i \rho' [\boldsymbol{V}(\boldsymbol{e}_i)(P_{\phi\phi})_{im} + \boldsymbol{U}_m(\boldsymbol{e}_i) \hat{\phi}_i] \rho \tag{12}$$

The rationale behind this combination of terms is hard to fathom, but again suppose that there is a good estimate of the modal state. The dominant term due to the discontinuity is simply $(\mathrm{d}/\mathrm{d}t) \pi_{xx}(m) = \cdots \rho' \boldsymbol{U}_m(\boldsymbol{e}_k) \rho$, the square of the base-state jump $(\rho', \ldots, \rho)$ times a factor related to its likelihood ($\boldsymbol{U}_m(\boldsymbol{e}_k)$).

The complexity of the PMEM algorithm is essentially that of the PME, and experience with the latter suggests that the computational requirements of Eq. (8) do not preclude its application.

III. Example

To illustrate the utility of PMEM in tracking an agile target, suppose an antiship missile is launched at a range of 80 km. The missile approaches the ship at nearly constant altitude and speed of 300 m/s. The target is detected at a range of slightly over 35 km. Soon after detection, the target makes a 6.5-g turn to the right while simultaneously translating 200 m in the Y direction. This motion is only an approximation to an actual missile path. Neither the change in angular rate nor the translation can be accomplished instantaneously. (A 200-m translation would require a 40-g acceleration even if achieved in 1 s.) Nevertheless, this singular motion is interesting as a demanding test for a tracking algorithm.

The position discontinuity accentuates the turn as seen from the ship. After turning for 6 s, the missile returns to the coast mode and reverses the discontinuity. This is a more complicated version of a portion of one of the motion paths created by investigators at the Naval Surface Warfare Center, Dahlgren Division, to provide realistic benchmark tests for proposed tracking algorithms.[16]

The sensor suite contains a phased array radar. The radar errors are Gaussian with standard deviation 40 m in range and 0.00175 rad in bearing (at 35 km this translates into about a 60-m cross-range error). The radar interdwell time is 2 s. Because the short duration of the turn, the radar has neither the update rate nor accuracy to clearly resolve it. The EKF selected for comparison is found by neglecting the maneuvers, i.e., $A \equiv A(\psi = 0)$, and its coefficients are based on the specification of radar quality given earlier. With the near constant speed of the target, $W = 1\ (\mathrm{m/s})^2$. The initial covariance is diagonal with standard deviation in position (100 m) and velocity (20 m/s). The EKF and the other estimators shown here are initialized on the true target motion at the time of detection, though the estimators do not know this. The small path noise (a standard deviation of about 0.1 g over a second) is actually conservative as compared to that used in the simulation. Improved performance in the turn can be achieved by selecting a larger value for W (pseudonoise), but this is accomplished at the expense of poorer path following during quiescent periods. (A bigger W gives a bigger gain and more amplification of the observation noise.) The PMEM that follows uses this same small value for W.

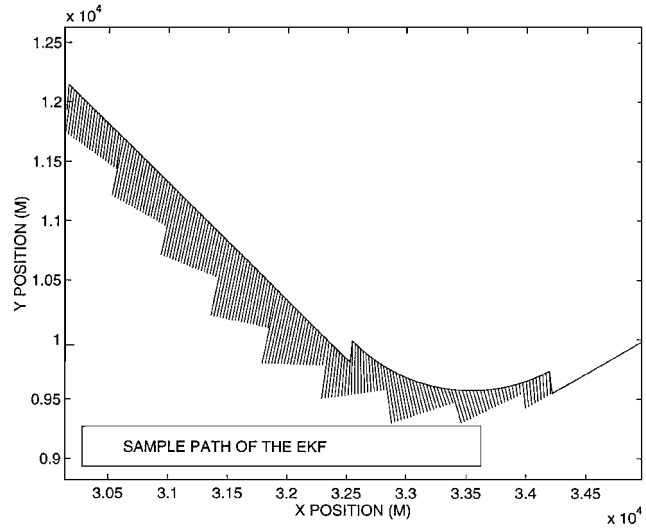

Fig. 1 Target path along with estimates of position generated by an EKF with interdwell interval 2 s.

A sample of a portion of the path beginning with detection is shown in Fig. 1 along with a feather plot of the output of the EKF. The feather plot is formed by linking the estimate of position generated by the EKF to the target path. From detection, the estimator has 3 s to initialize itself on the initial coast segment before beginning the first turn. The time of target detection is set at $t = 0$.

The EKF is not adequate in this application. Because of the omniscient initialization, the EKF tracks well into the first turn. The discontinuity at the turn is reflected immediately in the tracking error. The radar fix at $t = 4$ s improves things, but the EKF errors grow because the velocity has not been properly determined: the 80-m/sample radar error accumulates in the EKF to around 800 m. The radar modeled in Ref. 16 looses lock at about 400 m, and at this range the EKF would experience LOL. From Fig. 1, it is evident that the EKF has correctly determined the velocity near the end of the path, but the error is still quite large.

To illustrate the utility of modal augmentation, suppose this sensor suite is supplemented with an imager measuring both target orientation and maneuver mode. The quality of the orientation sensor/processor is delineated by the frame rate λ, the angular quantization L, and the discernibility matrix $\mathbf{P}$. It will be assumed that the modal sensor operates at a rate of $\lambda = 10$ measurements/s. For the purposes of this study, very coarse bins will be used: $L = 12$ (30-deg bins). Both the frame rate and the angular descretization are well within current practice.

The $\mathbf{P}$ matrix characterizes the fidelity of the modal sensor/processor for a single observation. A useful taxonomy separates the orientation errors into three categories. Local degradation could be caused by pixel noise and quantization. This will be represented by assuming that the orientation is misclassified symmetrically into a neighboring bin (spillover error, labeled NE). Other sources of measurement distortion act globally, e.g., severe occlusion. This results in errors of large magnitude and will be represented by assuming that the orientation is classified with uniform probability across all possible angular bins (labeled BE). The most distinctive orientation error occurs when the bin selected by the processor is symmetrically placed about a line perpendicular to the line of sight (labeled PE). This error source represents the intrinsic ambiguity that arises when the orientation classifier relies heavily on the silhouette of the extended object.

In addition to the orientation measurement, the PMEM can avail itself of a direct maneuver measurement. The translational acceleration may be noticeable from a peculiarity in measured image of the target, or the thruster may have a distinctive spectral resonance. Errors in maneuver classification (labeled ME) will be assumed to be uniform across the appropriate bins. The specific modal classifier

Table 1 Error rates for the modal sensor/processor

Modal error parameters	
Error type	Prob
BE	0.1
NE	0.1
PE	0.3
ME	0.2

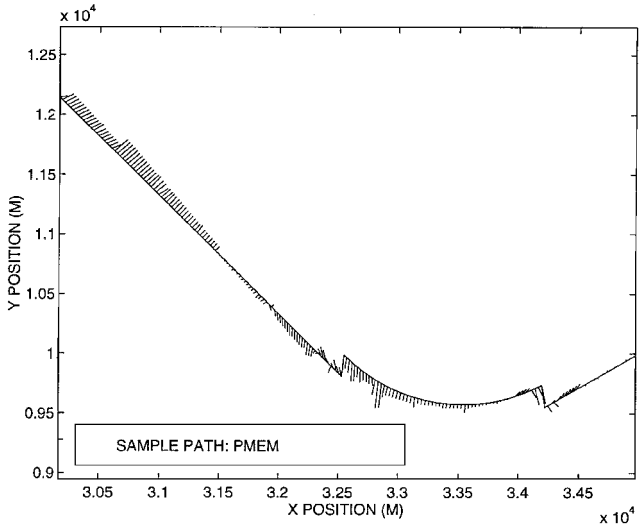

Fig. 2 Target path along with estimates of position generated by a PMEM with 2-s radar.

used in this example has the parameters shown in Table 1. It is possible to construct $\mathbf{P}$ from these (independent) primitives.

Although the standard deviation of the modal errors does not give a clear indication of measurement accuracy in the same way it does for the radar, it is interesting to compare the size of the angular errors for the two sensors. It the true target orientation is uniform in the bin, and if the projection error, which can vary from 0 to 180 deg, is set at 90 deg, the standard deviation of orientation classifier is 76 deg. This error is so big as to suggest the orientation classifier would be of little use in tracking (compare the radar bearing error of 0.1 deg).

The PMEM delineates the maneuver modes as follows. The set of turns is given by $\{\pm 0.2r/s, \alpha = \boldsymbol{e}_1, \boldsymbol{e}_3; 0r/s, \alpha = \boldsymbol{e}_2\}$. The mean sojourn time in each of the maneuver states will be assumed to be 5 s, with each turn being followed by a coast. From coast, the turns are equally likely. The initial maneuver modes will be assumed to be equally likely. From this the maneuver dynamics can be deduced.

Figure 2 shows the feather plot of the PMEM on the path using the same radar. Before the first turn, the PMEM is worse than the EKF: the EKF is oblivious of the possibility of a turn and will perform quite well if no turns occur. The PMEM recognized (with some delay) the turn and the associated discontinuity in position. As the turn progresses, the PMEM biases its error in the direction that will make the transition to coast easier. Therefore, the return to coast creates less error. As the coast proceeds, this sample function shows a small bias toward another right turn, but this is an artifact of the sample.

One reason the tracking error of an EKF for exceeds the radar error is that it improperly updates its location estimates. The error covariance calculated as part of the EKF is wrong: it is usually too small. Because the gains of the EKF are lower than they should be, the path correction during a turn is too small as well. (Of course, the EKF is also unable to resolve the change in velocity, and this is what leads to the slow return to quiescence during the second coast.) The PMEM uses a better algorithm for computing P_{XX}. Figure 3 displays a sample of the centered error ellipses generated by the EKF and the PMEM. The ellipses are formed from the computed values of P_{XX} and P_{YY} (and are shown only every 0.4 s) and are centered on the associated estimate. The error ellipses of the

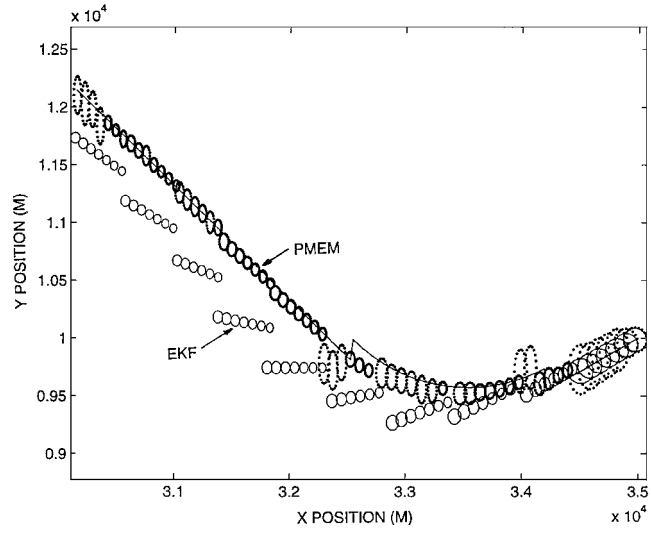

Fig. 3 Computed error ellipses for the EKF and the PMEM; ellipses for the EKF are the light curves, the ellipses for the PMEM are bold or dotted, depending on the scale.

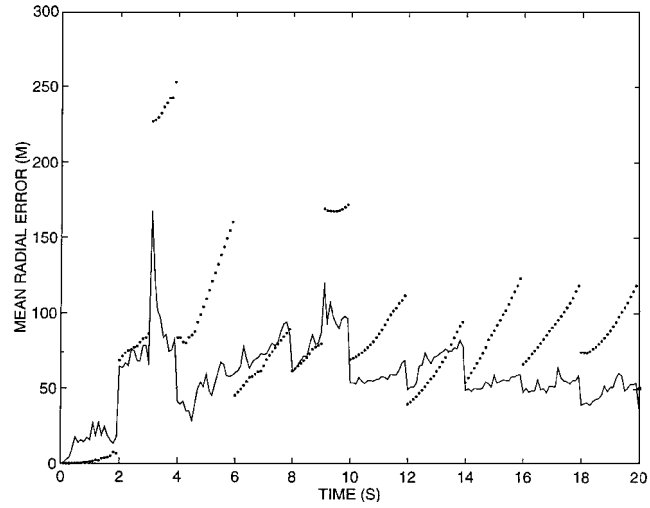

Fig. 4 Mean radial error: ——, PMEM and ·····, PME.

EKF are smaller than those of the PMEM. This indicates that the EKF imagines itself to be doing a good job. But the EKF is deluding itself. The true path is not within the 1σ ellipses after the turn begins, or the 2σ or even the 5σ in some cases. The PMEM, as befits its recognition of the uncertainty created by maneuvers, has larger ellipses, and in the main they encircle the true path. Note that, after the maneuver transition events, the PMEM error ellipses grow significantly. The computed error variance of the PMEM is thus responsive to changing conditions. Calculation of the error ellipses has importance that transcends this application. Adaptive trackers may adjust the SNR of the radar, the radar dwell interval, the radar window size, etc., in response to the computed error covariance. When P_{xx} is computed inaccurately, the adaptation may be unsuitable.

The PMEM is closely related to and is somewhat more complicated than the basic PME. The latter acknowledges the possibility of a turn but is blind to the path discontinuities. Figure 4 shows the mean radial tracking errors of the PMEM and a PME with the orientation errors given in Table 1. Figure 4 was generated as the sample average of 10 independent runs. The error values should not be over interpreted because of the small sample size. Because both of the trackers see the same observation sequence, the figure points clearly to their relative performance differences.

Certain aspects of the PMEM are apparent from Fig. 4. With perfect initialization, both PMEs begin with small error, but the basic PME is superior because it expects no jump changes and none

has occurred. (The increase in error at $t = 2$ s is created by a radar measurement moving both PMEs away from their omniscient initialization.) Both trackers have a unavoidable increase in error after the first turn, circa $t = 3$ s. The PMEM is better during the turn but not uniformly so. As the turn progresses, the PMEM biases its error to prepare for the return to coast. After the transition, circa $t = 9$ s, the PMEM is again far superior. Note that both of the PMEs keep their errors much closer to the 80-m radar error than does the EKF even though all of the trackers have a 2-s interdwell time.

IV. Conclusions

Novel measurement architectures hold promise for considerable improvement in estimator performance. An approximation to the best mean-square estimate of the state of a particular nonlinear system is derived. The estimator is based on a decomposition of the roles of two complementary measurement sources. An algorithm that increases its gains during times of modal uncertainty is quicker to respond during the posttransition intervals without simultaneously increasing amplification of the observation noise during quiescent periods. This modification of the PME demonstrates the even severe motion anomalies can be countered by improved modeling and sensor integration.

In the context of a demanding tracking problem, the following is shown.

1) Proper integration of modal measurements significantly improves tracking performance as compared to the conventional EKF.

2) The maximum tracking error using the PMEM is much smaller than that associated with a tracker that ignores the discontinuities (the PME).

3) The PMEM has a better idea of its own errors and, hence, is more suitable for use in an measurement-adaptive implementation.

4) The PMEM is somewhat more complicated than the PME, but the order of the recursion is the same.

Because of its special sensor structure, the PMEM cannot be implemented in every application, but when it can, it is worthy of consideration. In other studies (not shown), it has been determined that the performance using a conventional algorithm is inferior to the PMEM even if the radar update rate is increased by an order of magnitude. Improved response from the PMEM could be obtained with finer orientation bins at the expense of more online computation. The vignette selected in this study is at relatively long range. An ongoing study seeks the relative behavior of close-in target initialization, acquisition, and tracking.

Appendix: Derivation of the PME

Let $\{\boldsymbol{F}_t\}$ be a right-continuous filtration in a probability space $(\Omega, \boldsymbol{F}, \wp)$. All of the exogenous processes in what follows are adapted to $\boldsymbol{F}_t$ and the filtrations are contained in $\boldsymbol{F}$. The state of the target (x_t, ϕ_t) is associated with a similarly partitioned observation, $\text{vec}(y_t, \sigma_t) = g_t$. The $\boldsymbol{G}_t$ innovations process can be compatibly partitioned, $\nu_t = \text{vec}(\nu_x, \nu_\phi)$. To aid in the development, a simplified notation is useful. Let $h = \lambda \mathbf{P}'$. Then, $E\{\mathrm{d}\sigma \mid \boldsymbol{F}_t\} = h'\phi \,\mathrm{d}t$. The approximation to the $\boldsymbol{G}_t$ conditional expectation of $\{x_t, \phi_t\}$ used here is based on the premise that the primary source of information about ϕ_t is conveyed by $\{\sigma_t\}$: if $\{\varsigma_t\}$ is a process for which the $\hat{\boldsymbol{G}}_t$ expectation is independent of $\{y_t\}$, the contribution of $\mathrm{d}\nu_x$ to $\mathrm{d}\hat{\varsigma}_t$ is negligible as compared to that of $\mathrm{d}\nu_\phi$. Hence, $E\{\mathrm{d}\sigma \mid \boldsymbol{G}_t\} = h'\hat{\phi}_t \,\mathrm{d}t \cong E\{\mathrm{d}\sigma \mid \boldsymbol{Z}_t\}$. The modal observation has alternative decompositions: $\mathrm{d}\sigma = h'\hat{\phi}_t \,\mathrm{d}t + \mathrm{d}\nu_\phi$ and $\mathrm{d}\sigma = h'\phi_t \,\mathrm{d}t + \mathrm{d}n_\phi$, where $\{n_\phi\}$ is an $\boldsymbol{F}_t$ martingale and $\{\nu_\phi\}$ is a $\boldsymbol{Z}_t$ martingale. The predictable quadratic variation of $\{n_\phi\}$ is random: $\mathrm{d}\langle n_\phi, n'_\phi; \boldsymbol{F}_t\rangle = \text{diag}(h'\phi_t)\,\mathrm{d}t$; $\mathrm{d}\langle n_\phi, n'_\phi; \boldsymbol{Z}_t\rangle = \text{diag}(h'\hat{\phi}_t)\,\mathrm{d}t = R_\phi \,\mathrm{d}t$. The modal dynamics will be assumed to be such that $R_\phi > 0$. Define the vector observation rate $\boldsymbol{\lambda}_t = h'\phi_t$, and let $\{\vartheta_t\}$ be a process that is constant between modal observations with increments $\Delta\vartheta_t = h(\hat{\boldsymbol{\lambda}}_t^{-1} * \Delta\sigma_t)$. The modal-state estimator is given in Eq. (9) of Ref. 13 and can be written concisely as

$$\mathrm{d}\hat{\phi}_t = Q'\hat{\phi}_t \,\mathrm{d}t + \gamma_{\phi\phi} \,\mathrm{d}\nu_\phi \tag{A1}$$

where $\gamma_{\phi\phi} = P_{\phi\phi} h R_\phi^{-1}$ [$P_{\phi\phi} = \boldsymbol{G}_t - \text{Var}(\phi_t)$]. To determine the equation of evolution of the $\boldsymbol{G}_t$ conditional mean of $\{x_t\}$, a formalism will be employed, which was used successfully by Elliott[17] (see specifically Chap. 18). The basic approach is to find two particular representations of $E\{\mathrm{d}(\hat{x}_t g') \mid \boldsymbol{G}_t\}$. Because of the unique decomposition of the $\{\hat{x}_t g'_t\}$ process, the predictable compensators must be equal. From this, the innovations gain factor can be deduced. In what follows, the continuous measurement case is studied, i.e., the base-state observation is given in Eq. (3). The modification necessary for discrete observations is given at the end of the section.

The equations of evolution of $\{\hat{x}_t\}$ and three canonical higher moments, $P_{xx} = E\{\tilde{x}_t \tilde{x}'_t \mid \boldsymbol{G}_t\}$, $P_{x\phi} = E\{\tilde{x}_t \tilde{\phi}'_t \mid \boldsymbol{G}_t\}$, and $\pi_{xx}(m) = E\{\tilde{x}_t \tilde{x}'_t \tilde{\phi}_m \mid \boldsymbol{G}_t\}$ are as follows. Denote $R_{x\phi} = E\{x\phi' \mid \boldsymbol{G}_t\} = P_{x\phi} + \hat{x}\hat{\phi}'$.

Evolution of $\{\hat{x}_t\}$

Between modal observations,

$$\mathrm{d}\hat{x}_t = \left[\sum_i A_i (R_{x\phi})_{\cdot i} + \rho' Q' \hat{\phi}_t\right] \mathrm{d}t + \gamma_x \,\mathrm{d}\nu_x$$

At a modal observation,

$$\Delta\hat{x} = P_{x\phi}\Delta\vartheta \tag{A2}$$

Proof: Equation (1) can be written

$$\mathrm{d}x_t = \left(\sum_i A_i x_t \phi_i + \rho' Q' \phi_t\right) \mathrm{d}t + \sum_i B_i \phi_i \,\mathrm{d}w_t + \rho' \,\mathrm{d}m_t \tag{A3}$$

But

$$\sum_i B_i \phi_i \,\mathrm{d}w_t + \rho' \,\mathrm{d}m_t$$

is an $\boldsymbol{F}_t$-martingale increment. Let

$$\sum_i A_i x_t \phi_i + \rho' Q' \phi_t = F_x$$

It is a direct exercise to show $\mathrm{d}\hat{x}_t = \hat{F}_x \,\mathrm{d}t + \gamma_x \,\mathrm{d}\nu_x + \gamma_\phi \,\mathrm{d}\nu_\phi$ subject to $\gamma_\phi = P_{x\phi} h R_\phi^{-1}$ (Ref. 18). Simplifying, Eq. (A2) follows. □

Moment Properties of $\{\boldsymbol{m}_t\}$ and $\{\boldsymbol{n}_t\}$

To obtain the required moments for $\{x_t, \phi_t\}$, it is helpful to have some of the moment equations for the exogenous disturbances. These are found by enumerating the alternatives and computing the required conditional expectations.

1) For $E\{\mathrm{d}m \,\mathrm{d}m' \mid \boldsymbol{F}_t\}$,

$$E\{\mathrm{d}m \,\mathrm{d}m' \mid \boldsymbol{F}_t\} = \mathrm{d}\langle m, m; \boldsymbol{F}_t\rangle$$

$$= [\text{diag}(Q'\phi) - (\text{diag}\,\phi)Q - Q'(\text{diag}\,\phi)]\,\mathrm{d}t = \boldsymbol{V}(\phi)\,\mathrm{d}t$$

where

$$\boldsymbol{V}(\phi) = \sum_i \boldsymbol{V}(\boldsymbol{e}_i)\phi_i$$

(Ref. 19). The $\boldsymbol{G}_t$ predictable quadratic variation of $\{m_t\}$ is

$$\mathrm{d}\langle m, m; \boldsymbol{G}_t\rangle = \sum_i \boldsymbol{V}(\boldsymbol{e}_i)\hat{\phi}_i \,\mathrm{d}t$$

2) For $E\{\mathrm{d}m \,\mathrm{d}m' \,\mathrm{d}m_k \mid \boldsymbol{F}_t\}$, let $E\{\mathrm{d}m \,\mathrm{d}m' \,\mathrm{d}m_k \mid \phi_t = e_r\} = \boldsymbol{U}_k(\boldsymbol{e}_r)\,\mathrm{d}t$. Then direct evaluation yields $\boldsymbol{U}_k(\boldsymbol{e}_r) = (\boldsymbol{e}_r - \boldsymbol{e}_k)Q_{rk}(\boldsymbol{e}_r - \boldsymbol{e}_k)' + \{\boldsymbol{e}_r \otimes (\boldsymbol{e}'_r Q) + [\boldsymbol{e}_r \otimes (\boldsymbol{e}'_r Q)]' - \text{diag}(\boldsymbol{e}'_r Q)\}\delta_{rk}$. Hence,

$$E\{\mathrm{d}m \,\mathrm{d}m' \,\mathrm{d}m_k \mid \boldsymbol{F}_t\} = \sum_r \boldsymbol{U}_k(\boldsymbol{e}_r)\phi_r \,\mathrm{d}t$$

$$E\{\mathrm{d}m \,\mathrm{d}m' \,\mathrm{d}m_k \mid \boldsymbol{G}_t\} = \sum_r \boldsymbol{U}_k(\boldsymbol{e}_r)\hat{\phi}_r \,\mathrm{d}t$$

3) For $E\{\mathrm{d}n_\phi \,\mathrm{d}n'_\phi(\mathrm{d}n_i) \mid \boldsymbol{F}_t\}$, by direct evaluation $E\{\mathrm{d}n_\phi \mathrm{d}n'_\phi \times (\mathrm{d}n_i) \mid \boldsymbol{F}_t\} = (h'\phi)_i \boldsymbol{E}_i \,\mathrm{d}t$. Hence, $E\{\mathrm{d}n_\phi \,\mathrm{d}n'_\phi \,(\mathrm{d}n_i) \mid \boldsymbol{G}_t\} = \hat{\lambda}_i \boldsymbol{E}_i \,\mathrm{d}t$.

The equation for P_{xx} involves a particular combination of canonical moments: $\Xi_2(i) = E\{(x\phi_i)\tilde{\ }\tilde{x}' \mid \boldsymbol{G}_t\} = \pi_{xx}(i) + P_{xx}\hat{\phi}_i + \hat{x}_t(P_{x\phi})'_{\cdot i}$.

Evolution of $\{P_{xx}\}$

The base-state error covariance satisfies the following equation. Between modal observations,

$$\frac{\mathrm{d}}{\mathrm{d}t}P_{xx} = \left[\sum_i A_i\,\Xi_2(i) + \rho' Q' P_{\phi x}\right] + [\cdots]' - \gamma_x R_x \gamma_x' + \sum_i W_i \hat{\phi}_i + \sum_r \rho' V(\boldsymbol{e}_r)\hat{\phi}_r \rho$$

At a modal observation,

$$\Delta P_{xx} = -\Delta\hat{x}\,\Delta\hat{x}' + \sum_k \pi_{xx}(k)\Delta\vartheta_k \tag{A4}$$

Proof: From Eqs. (1) and (A2), the base-state error satisfies

$$\mathrm{d}\tilde{x}_t = \left[\sum_i A_i(x\phi_i)\tilde{} + (\rho' Q' - \gamma_\phi h')\tilde{\phi} - \gamma_x D\tilde{x}\right]\mathrm{d}t - \gamma_x\,\mathrm{d}n_x - \gamma_\phi\,\mathrm{d}n_\phi + \sum_i B_i\phi_i\,\mathrm{d}w + \rho'\,\mathrm{d}m$$

The outer product of the base-state error can be expanded using $\mathrm{d}(\tilde{x}_t\tilde{x}_t') = (\mathrm{d}\tilde{x}_t)(\tilde{x}_t') + \tilde{x}_t(\mathrm{d}\tilde{x}_t') + (\mathrm{d}\tilde{x}_t)(\mathrm{d}\tilde{x}_t')$ to yield

$$\begin{aligned}\mathrm{d}(\tilde{x}_t\tilde{x}_t') &= \left\{\left[\sum_i A_i(x\phi_i)\tilde{} + (\rho' Q' - \gamma_\phi h')\tilde{\phi} - \gamma_x D\tilde{x}\right]\mathrm{d}t - \gamma_x\,\mathrm{d}n_x - \gamma_\phi\,\mathrm{d}n_\phi + \mathrm{d}w + \rho'\,\mathrm{d}m\right\}\tilde{x}_t' + \tilde{x}_t[\cdots]' \\ &\quad + \rho'\,\mathrm{d}m\,\mathrm{d}m'\rho + \gamma_\phi\,\mathrm{d}n_\phi(\mathrm{d}n_\phi)'\gamma_\phi' + \left(\gamma_x R_x\gamma_x' + \sum_i \phi_i W_i\right)\mathrm{d}t \\ &= F_{xx}\,\mathrm{d}t + \mathrm{d}\mu_t\end{aligned} \tag{A5}$$

where $\{F_{xx}\}$ is the $\boldsymbol{F}_t$ compensator of $\{\tilde{x}_t\tilde{x}_t'\}$ and $\{\mu_t\}$ is the (matrix) $\boldsymbol{F}_t$ martingale appropriate to the application. Because $\mathrm{d}(\tilde{x}_t\tilde{x}_t'\sigma_k) = \mathrm{d}(\tilde{x}_t\tilde{x}_t')\sigma_k + (\tilde{x}_t\tilde{x}_t')'(\mathrm{d}\sigma_k) + \mathrm{d}(\tilde{x}_t\tilde{x}_t')(\mathrm{d}\sigma_k)$, several groups of terms must be evaluated, e.g.,

$$\mathrm{d}(\tilde{x}_t\tilde{x}_t')(\mathrm{d}\sigma_k) = [(-\gamma_x\,\mathrm{d}n_x - \gamma_\phi\,\mathrm{d}n_\phi + \mathrm{d}w + \rho'\,\mathrm{d}m)\tilde{x}_t'\,\mathrm{d}n_k] + [\cdots]' + [\rho'\,\mathrm{d}m\,\mathrm{d}m'\rho + \gamma_\phi\,\mathrm{d}n_\phi(\mathrm{d}n_\phi)'\gamma_\phi']\,\mathrm{d}n_k$$

where only the martingale products have been retained and $(n_\phi)_k$ has been written n_k. But $\gamma_\phi\,\mathrm{d}n_\phi\tilde{x}'\,\mathrm{d}n_k = \gamma_\phi\boldsymbol{e}_k\,\mathrm{d}n_k\tilde{x}'$, so that

$$E\{\gamma_\phi\,\mathrm{d}n_\phi\tilde{x}'\,\mathrm{d}n_k \mid \boldsymbol{F}_t\} = \sum_j \gamma_\phi\boldsymbol{e}_k\tilde{x}'h_{kj}'\phi_j$$

Continuing,

$$E\{\gamma_\phi\,\mathrm{d}n_\phi\tilde{x}'\,\mathrm{d}n_k \mid \boldsymbol{G}_t\} = \sum_j \gamma_\phi\boldsymbol{e}_k h_{kj}'(P_{\phi x})_{j\cdot} = \gamma_\phi\boldsymbol{e}_k(h'P_{\phi x})_{k\cdot}$$

Further, $\mathrm{d}m\,\mathrm{d}n_k = 0$. Combining terms, $E\{\mathrm{d}(\tilde{x}_t\tilde{x}_t')(\mathrm{d}\sigma_i) \mid \boldsymbol{G}_t\} = -(\hat{\lambda})_i\gamma_\phi\boldsymbol{E}_i\gamma_\phi'$. Also, $\mathrm{d}(\tilde{x}_t\tilde{x}_t')(\sigma_i) = F_{xx}\sigma_i\,\mathrm{d}t + \mathrm{d}\mu$. Taking the expectation of this, $E\{\mathrm{d}(\tilde{x}_t\tilde{x}_t')(\sigma_i) \mid \boldsymbol{G}_t\} = \hat{F}_{xx}\sigma_i\,\mathrm{d}t$. Finally, $(\tilde{x}_t\tilde{x}_t')(\mathrm{d}\sigma_i) = (\tilde{x}_t\tilde{x}_t')[(\phi'h)_i\,\mathrm{d}t + \mathrm{d}n_i]$. Taking the expectation of this, and nothing that $E\{(\tilde{x}_t\tilde{x}_t')(\mathrm{d}n_i) \mid \boldsymbol{G}_t\} = 0$, it follows that

$$E\{(\tilde{x}_t\tilde{x}_t')(\mathrm{d}\sigma_i) \mid \boldsymbol{G}_t\} = \sum_k [\pi_{xx}(k) + P_{xx}\hat{\phi}_k]h_{ki}\,\mathrm{d}t$$

Combining,

$$E\{\mathrm{d}(\tilde{x}_t\tilde{x}_t'\sigma_i) \mid \boldsymbol{G}_t\} = \left\{-(h'\hat{\phi}_t)_i\gamma_\phi\boldsymbol{E}_i\gamma_\phi' + \hat{F}_{xx}\sigma_i + \sum_k [\pi_{xx}(k) + P_{xx}\hat{\phi}_k]h_{ki}\right\}\mathrm{d}t$$

If the $\boldsymbol{G}_t$ innovations associated with $\{y_t\}$ are small, P_{xx} has the representation

$$\mathrm{d}P_{xx} = \hat{F}_{xx}\,\mathrm{d}t + \sum_{m\in\boldsymbol{S}} \gamma_{xx}(m)\,\mathrm{d}\nu_m \tag{A6}$$

where $\mathrm{d}(\nu_\phi)_m = \mathrm{d}\nu_m$ and $\{\gamma_{xx}(m);\, m \in \boldsymbol{S}\}$ is a set of gains that must be determined. But $(\mathrm{d}P_{xx})(\mathrm{d}\sigma_i) = \gamma_{xx}(i)\,\mathrm{d}n_i$. Taking the expectation of this, $E\{(\mathrm{d}P_{xx})(\mathrm{d}\sigma_i) \mid \boldsymbol{G}_t\} = \gamma_{xx}(i)(h'\hat{\phi})_i\,\mathrm{d}t$. From Eq. (A6), it follows directly that $E\{(\mathrm{d}P_{xx})(\sigma_i) \mid \boldsymbol{G}_t\} = \hat{F}_{xx}\sigma_i\,\mathrm{d}t$. Further, $E\{(P_{xx})(\mathrm{d}\sigma_i) \mid \boldsymbol{G}_t\} = P_{xx}(h'\hat{\phi})_i\,\mathrm{d}t$. Combining, $E\{\mathrm{d}(P_{xx}\sigma_i) \mid \boldsymbol{G}_t\} = \{[\gamma_{xx}(i) + P_{xx}](h'\hat{\phi})_i + \hat{F}_{xx}\sigma_i\}\,\mathrm{d}t$. Because the compensators of $P_{xx}\sigma_i$ must be equal,

$$[\gamma_{xx}(i) + P_{xx}](h'\hat{\phi})_i + \hat{F}_{xx}\sigma_i = -(h'\hat{\phi}_t)_i\gamma_\phi\boldsymbol{E}_i\gamma_\phi' + \hat{F}_{xx}\sigma_i + \sum_k [\pi_{xx}(k) + P_{xx}\hat{\phi}_k]h_{ki}$$

or

$$\gamma_{xx}(i) = \hat{\lambda}_i^{-1}\left\{-\gamma_\phi\boldsymbol{E}_i[(h'\hat{\phi}_t)_i]\gamma_\phi' + \sum_k \pi_{xx}(k)h_{ki}\right\}$$

The innovations term in Eq. (A6) can now be written:

$$\sum_{i\in\boldsymbol{S}} \gamma_{xx}(i)\,\mathrm{d}\nu_i = -\sum_i \gamma_\phi\boldsymbol{E}_i\gamma_\phi'\,\mathrm{d}\nu_i + \sum_i \pi_{xx}(i)\left(hR_\phi^{-1}\mathrm{d}\nu_\phi\right)_i$$

Note that, between jumps in $\{\sigma_t\}$,

$$\sum_{i\in\boldsymbol{S}} \gamma_{xx}(i)\,\mathrm{d}\nu_i = -\gamma_\phi R_\phi\gamma_\phi'\,\mathrm{d}t$$

To complete the equation for P_{xx}, $\hat{F}_{xx}$ must be evaluated explicitly. Doing this and combining as was done in Ref. 18, Eq. (A4) follows. □

The equation for $P_{x\phi}$ involves two additional combinations of the canonical moments:

$$\pi_{x\phi}(m) = E\{\tilde{x}\tilde{\phi}'\tilde{\phi}_m \mid \boldsymbol{G}_t\} = (P_{x\phi})_{\cdot m}\boldsymbol{e}_m' - \hat{\phi}_m P_{x\phi} - (P_{x\phi})_{\cdot m}\hat{\phi}'$$

$$\Xi_4(i) = E\{(x\phi_i)\tilde{}\,\tilde{\phi}' \mid \boldsymbol{G}_t\} = \pi_{x\phi}(i) + P_{x\phi}\hat{\phi}_i + \hat{x}_t(P_{\phi\phi})_{\cdot i}'$$

This development is fundamentally the same as that for P_{xx}.

Evolution of $\{P_{x\phi}\}$

The mixed (base state, modal state) central cross moment $P_{x\phi}$ satisfies the following.

Between modal observations,

$$\frac{\mathrm{d}}{\mathrm{d}t}P_{x\phi} = \sum_i A_i\,\Xi_4(i) + \rho' Q' P_{\phi\phi} - \gamma_x R_x\gamma_\phi' + P_{x\phi}Q + \sum_r \rho' V(\boldsymbol{e}_r)\hat{\phi}_r$$

At a modal observation,

$$\Delta P_{x\phi} = -\Delta\hat{x}\,\Delta\hat{\phi}' + \sum_{k\in\boldsymbol{S}} \pi_{x\phi}(k)\Delta\vartheta_k \tag{A7}$$

Proof: From Eqs. (2) and (A1), the modal-state error satisfies

$$\mathrm{d}\tilde{\phi}_t = Q'\tilde{\phi}_t\,\mathrm{d}t + \mathrm{d}m - \gamma_{\phi\phi}\,\mathrm{d}\nu_\phi \tag{A8}$$

The product of $(\mathrm{d}\tilde{x}_t)(\mathrm{d}\tilde{\phi}_t')$ is

$$\begin{aligned}(\mathrm{d}\tilde{x}_t)(\mathrm{d}\tilde{\phi}_t') &= \left\{\left[\sum_i A_i(x\phi_i)\tilde{} - \gamma_\phi h'\tilde{\phi} - \gamma_x D\tilde{x}\right]\mathrm{d}t - \gamma_x\,\mathrm{d}n_x - \gamma_\phi\,\mathrm{d}n_\phi + \sum_i B_i\phi_i\,\mathrm{d}w + \rho'\mathrm{d}m\right\}[(Q' - \gamma_{\phi\phi}h')\tilde{\phi}_t\,\mathrm{d}t \\ &\quad - \gamma_{\phi\phi}\,\mathrm{d}n_\phi + \mathrm{d}m]' = \gamma_\phi\,\mathrm{d}n_\phi\,\mathrm{d}n_\phi'\gamma_{\phi\phi}' + \rho'\,\mathrm{d}m\,\mathrm{d}m'\end{aligned}$$

Further substitution yields

$$\tilde{x}_t(\mathrm{d}\tilde{\phi}_t')=\tilde{x}_t[(Q'-\gamma_{\phi\phi}h')\tilde{\phi}_t\,\mathrm{d}t-\gamma_{\phi\phi}\,\mathrm{d}n_\phi+\mathrm{d}m]'$$

$$(\mathrm{d}\tilde{x}_t)\tilde{\phi}_t'=\left\{\left[\sum_i A_i(x\phi_i)\tilde{}-\gamma_\phi h'\tilde{\phi}-\gamma_x D\tilde{x}\right]\mathrm{d}t\right.$$

$$\left.-\gamma_x\,\mathrm{d}n_x-\gamma_\phi\,\mathrm{d}n_\phi+\sum_i B_i\phi_i\,\mathrm{d}w+\rho'\,\mathrm{d}m\right\}\tilde{\phi}_t'$$

Therefore, it follows that

$$\mathrm{d}(\tilde{x}_t\tilde{\phi}_t')=\left\{\left[\sum_i A_i(x\phi_i)\tilde{}-\gamma_\phi h'\tilde{\phi}-\gamma_x D\tilde{x}\right]\mathrm{d}t-\gamma_x\,\mathrm{d}n_x\right.$$

$$\left.-\gamma_\phi\,\mathrm{d}n_\phi+\sum_i B_i\phi_i\,\mathrm{d}w+\rho'\,\mathrm{d}m\,\mathrm{d}m_\ell\right\}(\tilde{\phi}_t')$$

$$+\tilde{x}_t[(Q'-\gamma_{\phi\phi}h')\tilde{\phi}_t\,\mathrm{d}t-\gamma_{\phi\phi}\,\mathrm{d}n_\phi+\mathrm{d}m]'$$

$$+\gamma_\phi\,\mathrm{d}n_\phi\,\mathrm{d}n_\phi'\gamma_{\phi\phi}'+\rho'\,\mathrm{d}m\,\mathrm{d}m'=F_{x\phi}\,\mathrm{d}t+\mathrm{d}\mu_t \tag{A9}$$

where $F_{x\phi}$ is the $\boldsymbol{F}_t$ compensator of $\{\tilde{x}_t\tilde{\phi}_t\}$ and $\{\mu_t\}$ is a matrix $\boldsymbol{F}_t$ martingale. But

$$\mathrm{d}(\tilde{x}_t\tilde{\phi}_t')(\mathrm{d}\sigma_k)=[-\gamma_\phi\,\mathrm{d}n_\phi\tilde{\phi}'+\tilde{x}_t(-\gamma_{\phi\phi}\,\mathrm{d}n_\phi)'+\gamma_\phi\,\mathrm{d}n_\phi\,\mathrm{d}n_\phi'\gamma_{\phi\phi}']\,\mathrm{d}n_k$$

Combining terms,

$$E\{\mathrm{d}(\tilde{x}_t\tilde{\phi}_t')(\mathrm{d}\sigma_k)\mid\boldsymbol{G}_t\}$$

$$=-y_\phi\boldsymbol{e}_k(h'P_{\phi\phi})_{k\cdot}-(P_{x\phi}h)_{\cdot k}\boldsymbol{e}_i'\gamma_{\phi\phi}+\gamma_\phi\boldsymbol{E}_k\hat{\lambda}_k\gamma_{\phi\phi}$$

Following the preceding development,

$$E\{\mathrm{d}(\tilde{x}_t\tilde{\phi}_t'\sigma_i)\mid\boldsymbol{G}_t\}=\left\{-\gamma_\phi\boldsymbol{e}_i(h'P_{\phi\phi})_{i\cdot}-(P_{x\phi}h)_{\cdot i}\boldsymbol{e}_i'\gamma_{\phi\phi}\right.$$

$$\left.+\gamma_\phi\boldsymbol{E}_i\hat{\lambda}_i\gamma_{\phi\phi}+\hat{F}_{x\phi}\sigma_i+\sum_k[\pi_{x\phi}(k)+P_{x\phi}\tilde{\phi}_k]h_{ki}\right\}\mathrm{d}t$$

Again using the assumption that the $\boldsymbol{G}_t$ innovations associated with $\{y_t\}$ is small,

$$\mathrm{d}P_{x\phi}=\hat{F}_{x\phi}\,\mathrm{d}t+\sum_{m\in\boldsymbol{S}}\gamma_{x\phi}(m)\,\mathrm{d}\nu_m \tag{A10}$$

where $\{\gamma_{x\phi}(m);\,m\in\boldsymbol{S}\}$ are a set of gains, which must be determined. Because the compensators of $P_{x\phi}\sigma_i$ must be equal,

$$\gamma_{x\phi}(i)=\hat{\lambda}_i^{-1}\left[-\gamma_\phi\boldsymbol{E}_i\hat{\lambda}_i\gamma_{\phi\phi}'+\sum_k\pi_{x\phi}(k)h_{ki}\right]$$

Note that

$$\sum_i\hat{\lambda}_i^{-1}\sum_k\pi_{x\phi}(k)\,h_{ki}\,\mathrm{d}\nu_i=\sum_{ki}\pi_{x\phi}(k)h_{ki}\hat{\lambda}_i^{-1}\,\mathrm{d}\nu_i$$

$$=\sum_k\pi_{x\phi}(k)\left(hR_\phi^{-1}\,\mathrm{d}\nu_\phi\right)_k$$

The innovations term can now be written as

$$\sum_{i\in\boldsymbol{S}}\gamma_{x\phi}(i)\,\mathrm{d}\nu_i=-\sum_i\gamma_\phi\boldsymbol{E}_i\gamma_{\phi\phi}'\,\mathrm{d}\nu_i+\sum_i\pi_{x\phi}(i)\left(hR_\phi^{-1}\,\mathrm{d}\nu_\phi\right)_i$$

Between jumps in $\{\sigma_t\}$,

$$\sum_{i\in\boldsymbol{S}}\gamma_{xx}(i)\,\mathrm{d}\nu_i=-\gamma_\phi R_\phi\gamma_{\phi\phi}'\,\mathrm{d}t$$

Combining and simplifying yields Eq. (A7). □

Calculation $\{\pi_{xx}(i),\,i\in\boldsymbol{S}\}$ entails more detail than that found in the second moments. However, the underlying procedure is the same. The third of the canonical moments requires the following identities:

$$\Phi_m(r)=E\{\tilde{x}\tilde{x}'\tilde{\phi}_r\tilde{\phi}_m\mid\boldsymbol{G}_t\}$$

$$=(\delta_{rm}-\hat{\phi}_r)\pi_{xx}(m)-\hat{\phi}_m\pi_{xx}(r)+P_{xx}(\hat{\phi}_r\delta_{rm}-\hat{\phi}_r\hat{\phi}_m)$$

$$\Xi_5(i,m)=E\{(x\phi_i)\tilde{}\,\tilde{x}'\tilde{\phi}_m\mid\boldsymbol{G}_t\}$$

$$=\Phi_i(m)+\hat{\phi}_i\pi_{xx}(m)+\hat{x}[\pi_{\phi x}(m)]_{i\cdot}-(P_{x\phi})_{\cdot i}(P_{\phi x})_{m\cdot}$$

Evolution of $\{\pi_{xx}(m)\}$

The third central mixed (base state, base state, modal state) $\pi_{xx}(m)$ satisfies the following.

Between modal observations,

$$\frac{\mathrm{d}}{\mathrm{d}t}\pi_{xx}(m)$$

$$=\left[\sum_i A_i\,\Xi_5(i,m)+\rho'Q'\pi_{\phi x}(m)-\gamma_x D\pi_{xx}(m)\right]+[\cdots]'$$

$$+\sum_r[\pi_{xx}(r)Q_{rm}+(P_{\phi\phi})_{rm}W_r]+\sum_r\rho'[\boldsymbol{V}(\boldsymbol{e}_r)(P_{\phi\phi})_{rm}$$

$$+\boldsymbol{U}_m(\boldsymbol{e}_r)\hat{\phi}_r]\rho+\left[\sum_r\rho'\boldsymbol{V}(\boldsymbol{e}_r)_{\cdot m}(P_{\phi x})_{r\cdot}\right]+[\cdots]'$$

At a modal observation,

$$\Delta\pi_{xx}(m)=-\Delta\hat{\phi}_m\Delta\hat{x}\Delta\hat{x}'-\Delta\hat{\phi}_m P_{xx}^+-\Delta\hat{x}\left(P_{\phi x}^+\right)_{m\cdot}$$

$$-\left[\Delta\hat{x}\left(P_{\phi x}^+\right)_{m\cdot}\right]'+\sum_j\Phi_m(j)\Delta\vartheta(j) \tag{A11}$$

Proof: Using the usual methods, the equation of evolution of $\tilde{x}_t\tilde{x}_t'\tilde{\phi}_m$ is

$$\mathrm{d}(\tilde{x}_t\tilde{x}_t'\tilde{\phi}_m)=[-\gamma_\phi\,\mathrm{d}n_\phi(-\gamma_{\phi\phi}\,\mathrm{d}n_\phi)_m+\rho'\,\mathrm{d}m\,\mathrm{d}m_m]\tilde{x}_t'+\tilde{x}_t[\cdots]'$$

$$+\rho'\,\mathrm{d}m\,\mathrm{d}m'\rho\,\mathrm{d}m_m+\gamma_\phi\,\mathrm{d}n_\phi(\mathrm{d}n_\phi)'\gamma_\phi'(-\gamma_{\phi\phi}\,\mathrm{d}n_\phi)_m$$

$$+\left(\left\{\left[\sum_i A_i(x\phi_i)\tilde{}+(\rho'Q'-\gamma_\phi h')\tilde{\phi}-\gamma_x D\tilde{x}\right]\mathrm{d}t\right.\right.$$

$$\left.-\gamma_x\,\mathrm{d}n_x\gamma_\phi\,\mathrm{d}n_\phi+\sum_i B_i\phi_i\,\mathrm{d}w+\rho'\,\mathrm{d}m\right\}\tilde{x}_t'$$

$$+\tilde{x}_t[\cdots]'+\rho'\,\mathrm{d}m\,\mathrm{d}m'\rho+\gamma_\phi\,\mathrm{d}n_\phi(\mathrm{d}n_\phi)'\gamma_\phi'$$

$$+\left(\gamma_x R_x\gamma_x'+\sum_i W_i\phi_i\right)\mathrm{d}t\Bigg)\tilde{\phi}_m$$

$$+(\tilde{x}_t\tilde{x}_t')[(Q'-\gamma_{\phi\phi}h')\tilde{\phi}_t\,\mathrm{d}t-\gamma_{\phi\phi}\,\mathrm{d}n_\phi+\mathrm{d}m]_m$$

$$=F_{xxm}\,\mathrm{d}t+\mathrm{d}\mu_t \tag{A12}$$

where F_{xxm} is the $\boldsymbol{F}_t$ compensator of $\{\tilde{x}\tilde{x}'\tilde{\phi}_m\}$ and $\{\mu_t\}$ is a matrix $\boldsymbol{F}_t$ martingale. Following the usual procedure,

$$E\{\mathrm{d}(\tilde{x}_t\tilde{x}_t'\tilde{\phi}_m)\,\mathrm{d}\sigma_k\mid\boldsymbol{G}_t\}=2(\gamma_{\phi\phi})_{mk}(\hat{\lambda}_k)\gamma_\phi\boldsymbol{e}_k\boldsymbol{e}_k'\gamma_\phi'$$

$$-\gamma_\phi\boldsymbol{e}_k\boldsymbol{e}_k'[h'(\phi\tilde{x}\tilde{\phi}_m)\hat{}\,]-\{\gamma_\phi\boldsymbol{e}_k\boldsymbol{e}_k'[h'(\phi\tilde{x}\tilde{\phi}_m)\hat{}\,]\}'$$

$$-(\gamma_{\phi\phi})_{mk}\sum_\alpha h_{\alpha k}[\pi_{xx}(\alpha)+\hat{\phi}_\alpha P_{xx}]$$

Again we have the representation

$$\mathrm{d}\pi_{xx}(m)=\hat{F}_{xxm}\,\mathrm{d}t+\sum_j\gamma_{xxm}(j)\,\mathrm{d}\nu_j$$

But

$$E\{[\mathrm{d}\pi_{xx}(m)]\,\mathrm{d}\sigma_k\mid\boldsymbol{G}_t\}=\{[\gamma_{xxm}(k)+\pi_{xx}(m)](h'\hat{\phi})_k+\hat{F}_{xxm}\sigma_k\}\,\mathrm{d}t$$

Combining and solving for the gain,

$$\gamma_{xxm}(k) = (h'\hat{\phi})_k^{-1}\Big\{2(\gamma_{\phi\phi})_{mk}(\hat{\lambda}_k)\gamma_\phi \boldsymbol{e}_k\boldsymbol{e}_k'\gamma_\phi' - \gamma_\phi \boldsymbol{e}_k\boldsymbol{e}_k' h'(\phi\tilde{x}\tilde{\phi}_m)\hat{} - [\gamma_\phi \boldsymbol{e}_k\boldsymbol{e}_k' h'(\phi\tilde{x}\tilde{\phi}_m)\hat{}]' - (\gamma_{\phi\phi})_{mk}\sum_\alpha h_{\alpha k}[\pi_{xx}(\alpha) + \hat{\phi}_\alpha P_{xx}] + \sum_j \Phi_m(j)h_{jk}\Big\}$$

Evaluating $\hat{F}_{xxm}\,\mathrm{d}t = E\{\mathrm{d}(\tilde{x}_t\tilde{x}_t'\tilde{\phi}_m)|\,\boldsymbol{G}_t\}$ and simplifying yields (A11). □

When the base-state measurement is discrete, the update can be formally determined as is done in the discrete KF: extrapolation terms involving γ_x are neglected and base-state updates use the γ_x terms in the extrapolation with R_x replaced with $(D P_{xx} D' + R_x)$. These substitutions yield the discrete PMEM used in the example.

References

[1]Maybeck, P. S., *Stochastic Models, Estimation, and Control*, Vol. 2, Academic, New York, 1982, Chap. 9.

[2]Singer, R. A., "Estimating Optimal Tracking Filter Performance for Manned Maneuvering Targets," *IEEE Transactions on Aerospace and Electronic Systems*, Vol. AES-10, July 1970, pp. 473–482.

[3]Maybeck, P. S., and Stevens, R. D., "Reconfigurable Flight Control Via Multiple Model Adaptive Control Methods," *IEEE Transactions on Aerospace and Electronic Systems*, Vol. AES-27, May 1991, pp. 470–480.

[4]Blom, H. A. K., and Bar-Shalom, Y., "The Interacting Multiple Model Algorithm for Systems with Markovian Switching Coefficients," *IEEE Transactions on Automatic Control*, Vol. AC-33, Aug. 1988, pp. 780–783.

[5]Daeipour, E., Bar-Shalom, Y., and Li, X., "Adaptive Beam Pointing Control of a Phased Array Radar Using an IMM Estimator," *Proceedings of the 1994 American Control Conference*, American Control Council, New York, pp. 2093–2097.

[6]Miller, M. I., Srivastava, A., and Grenander, U., "Conditional-Mean Estimation Via Jump-Diffusion Processes in Multiple Target Tracking/Recognition," *IEEE Transactions on Signal Processing*, Vol. 43, Nov. 1995, pp. 2678–2690.

[7]Sworder, D. D., Singer, P. F., Doria, D., and Hutchins, R. G., "Image Enhanced Estimation Methods," *IEEE Proceedings*, Vol. 81, No. 6, 1993, pp. 797–812.

[8]Pao, L. C., "Multisensor Multitarget Mixture Reduction Algorithms for Tracking," *Journal of Guidance, Control, and Dynamics*, Vol. 17, No. 6, 1994, pp. 1205–1211.

[9]Friedland, B., *Advanced Control System Design*, Prentice–Hall, Englewood Cliffs, NJ, 1995, pp. 314–324.

[10]Cloutier, J. R., Evers, J. H., and Feeler, J. J., "Assessment of Air-to-Air Missile Guidance and Control Technology," *IEEE Control Systems Magazine*, Vol. 9, Oct. 1989, pp. 27–34.

[11]Moose, R. L., Vanlandingham, V. F., and McCabe, D. H., "Modeling and Estimation for Tracking Maneuvering Targets," *IEEE Transactions on Aerospace and Electronics Systems*, Vol. AES-15, May 1979, pp. 448–455.

[12]Ricker, G. G., and Williams, J. R., "Adaptive Tracking Filter for Maneuvering Targets," *IEEE Transactions on Aerospace and Electronic Systems*, Vol. AES-14, No. 1, 1978, pp. 185–193.

[13]Sworder, D. D., Vojak, R., and Hutchins, R. G., "Gain Adaptive Tracking," *Journal of Guidance, Control, and Dynamics*, Vol. 16, No. 5, 1993, pp. 865–873.

[14]Sworder, D. D., and Hutchins, R. G., "Image-Enhanced Tracking," *IEEE Transactions on Aerospace and Electronic Systems*, Vol. AES-25, No. 5, 1989, pp. 701–710.

[15]Andrisani, D., Kim, E. T., Schierman, J., and Kuhl, F. P., "A Nonlinear Helicopter Tracker Using Attitude Measurements," *IEEE Transactions on Aerospace and Electronic Systems*, Vol. AES-27, Jan. 1991, pp. 40–47.

[16]Blair, W. D., Watson, G. A., and Hoffman, S. A., "Benchmark Problem for Beam Pointing Control of Phased Array Radar Against Maneuvering Targets," *Proceedings of the 1994 American Control Conference*, American Control Council, New York, pp. 2071–2075.

[17]Elliott, R. J., *Stochastic Calculus and Applications*, Springer–Verlag, New York, 1982, pp. 271–294.

[18]Sworder, D. D., and Vojak, R., "Hybrid Estimation Algorithms," *Journal of Optimization Theory and Applications*, Vol. 81, No. 1, 1994, pp. 143–167.